HOKKAIDO UNIVERSITY

Title	Preparation of europium-activated SrAl2O4 glass composites using the frozen sorbet technique
Author(s)	Nakanishi, Takayuki
Citation	Journal of the Ceramic Society of Japan, 123(1441), 862-867 https://doi.org/10.2109/jcersj2.123.862
Issue Date	2015-09
Doc URL	https://hdl.handle.net/2115/60218
Type	journal article
File Information	Nakanishi-JCSJ123(9).pdf

Hokkaido University Collection of Scholarly and Academic Papers : HUSCAP

Journal of the Ceramic Society of Japan 123 [9] 862-867 2015 Special Article
The 69th CerSJ Awards for Advancements in Ceramic Science and Technology: Review

Preparation of europium-activated $SrAl_2O_4$ glass composites using the frozen sorbet technique

Takayuki NAKANISHI†

Faculty of Engineering, Hokkaido University, Kita-13 Nishi-8, Kita-ku, Sapporo 060–8628, Japan

Unique photo-functionalities of luminescent Eu, Dy: $SrAl_2O_4$ glass ceramics with high transparency prepared by using the frozen sorbet technique are briefly reviewed. The crystal–glass composites have remarkable light-storage ability (e.g., charge-carrier trapping) based on the properties of $SrAl_2O_4$ crystals, and these provide characteristic photo-functionalities such as long-persistent luminescence and mechanoluminescence. In this review, the specific preparation of transparent $SrAl_2O_4$ glass composites using the frozen sorbet technique and their optical properties are described as novel light-storage materials for energy applications.

©2015 The Ceramic Society of Japan. All rights reserved.

Key-words : Europium, Frozen sorbet, Luminescence

[Received May 11, 2015; Accepted July 7, 2015]

1. Introduction

Lanthanide-doped luminescent materials are promising candidates as phosphors for solid-state lighting,[1] wavelength converters for solar cells,[2] electro-luminescence materials (EL) for display,[3] and scintillator materials for radiation detectors.[4] In recent years, the design and synthesis of inorganic materials with light-storage ability have received considerable attention for future photo-science and technology.[5)–9)] Some lanthanide-doped oxides (e.g., aluminates and silicates) show characteristic luminescence and electronic properties related to the light storage phenomenon.[10)–14)] For example, notable long-persisting luminescence of Eu^{2+} and Dy^{3+}-codoped $SrAl_2O_4$ crystals, the best persistent phosphor in the twentieth century, was reported by Matsuzawa et al[15] and had a great impact worldwide. In 2005, Clabau[10),11)] and Dorenbos[16] reviewed several mechanisms of long-persistent luminescence linked with the light-storage phenomenon of Eu^{2+}, Dy^{3+}: $SrAl_2O_4$. In addition, various improvements of lanthanide-doped $SrAl_2O_4$ crystals have been explored and their characteristic photo-physical properties have been studied.[17)–19)] The development of effective light-storage materials, i.e., Eu^{2+}, Dy^{3+}: $SrAl_2O_4$, is expected to open up a new field of novel inorganic chemistry in advanced opto-materials.

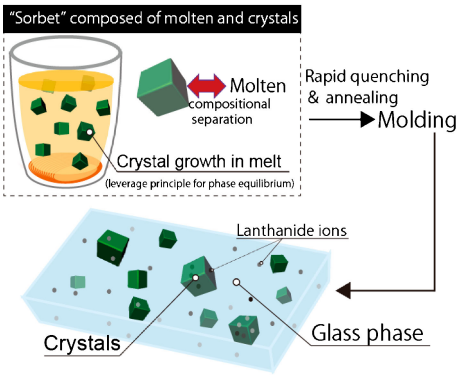
This review introduces the specific preparation of $SrAl_2O_4$ glass composites using the frozen sorbet technique[20),21)] to obtain applicative light-storage glass materials.[22),23)] $SrAl_2O_4$ micro-crystals are generated in SrO–Al_2O_3–B_2O_3 melt at around 1500°C under a weak reducing atmosphere. The dispersed particles of $SrAl_2O_4$ crystals are almost all mono-crystals and show notable light-storage properties related to crystal growth in the melt. As described later, the frozen sorbet technique is suitable for the synthesis of glass composites including desirable crystals with high-melting temperatures, such as α-Al_2O_3 (ruby) phase (>2050°C),[24] $Y_3Al_5O_{12}$ (YAG) phase (>1800°C)[25] and β-$CaSi_2O_4$ phase (>2100°C).[20] This review paper is organized as follows. In Section 2, the frozen sorbet technique is briefly described. The common feature of preparation is controlled crystallization of a target crystal by carefully studying related phase diagrams. In Section 3, structural features of $SrAl_2O_4$ glass composites obtained by using the frozen sorbet technique are described. In Section 4, unique photo-functional properties after light storage including novel results for elastico-mechanoluminescence are described. The advantages of $SrAl_2O_4$ glass composites are 1) transparency in the visible region, 2) unique photo-functionalities as luminescent materials and 3) easy preparation process. The hardness and chemical stability of crystal glass composites are also suitable for opto-electrical power devices. The transparent $SrAl_2O_4$ glass composites are expected to be applicable as light-storage materials for future energy generation technology.

2. Frozen sorbet technique: preparation of crystal–glass composites

It is well known that europium- (or cerium-) doped inorganic phosphor materials[26)–29)] exhibit characteristic luminescent properties based on their 4*f*–5*d* electro transition. In general, since these phosphors are prepared as a powder state composed of many micro-sized particles, a binder matrix of the organic polymers or resins is constantly required for optical applications. If crystal–glass composites including photo-functional crystals can be easily prepared as a bulk glass plate, the advantages of luminescent glass ceramics will lead to new photo-applications such as applications as light-storage materials. Glass ceramic processing is known as an excellent technique for the fabrication of functional materials with desired morphologies, and it is thus of interest to apply the glass crystallization method for fabrication of $SrAl_2O_4$ phosphors. However, it is known that precipitation of the single phase of $SrAl_2O_4$ through crystallization in glass is extremely difficult. Here, we can clearly distinguish between "glass ceramics" obtained by crystallization of glass and "crystal–glass composites" obtained by using the frozen sorbet method. In the latter case, the crystal–glass composites are prepared by quenching of mixtures (see **Scheme 1**). A "Sorbet state" at a moderate temperature below 0°C can be regarded as a mixture of ice (water solid) with a higher melting point and a water solution

† Corresponding author: T. Nakanishi; E-mail: nakanishi@eng.hokudai.ac.jp

©2015 The Ceramic Society of Japan
DOI http://dx.doi.org/10.2109/jcersj2.123.862



Scheme 1. Schematic for the frozen sorbet technique: preparation of crystal–glass composites.

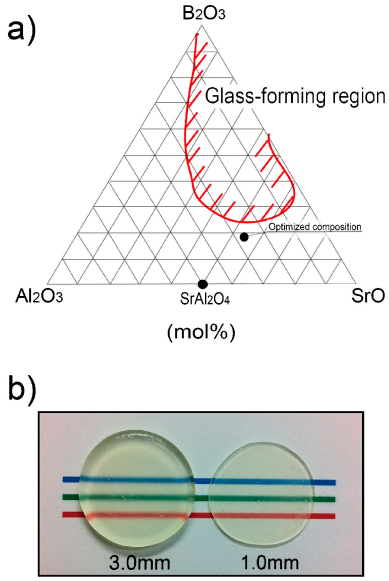


Fig. 1. Glass components and the glass-forming region on an SrO–Al_2O_3–B_2O_3 ternary compositional diagram and a picture of the obtained Eu and Dy-codoped $SrAl_2O_4$ crystal–glass composite. The thickness are 3 and 1 mm.

containing sugar and fruit juice with a lower liquidus temperature. This drop of liquidus temperature (melting point) is a result of a drop in the chemical potential of the solution, which keeps an equilibrium with the solid-state solvent, explained by well-known thermodynamics as "freezing point depression". In the frozen sorbet technique, for instance, the state of the melt consisting of liquid and crystalline phases of a given composition is often determined in accordance with the equilibrium phase diagram (i.e., leverage rule for phase equilibrium), a composite materials can therefore be designed or controlled more easily than they can when using a usual glass crystallization method. The main advantages are as follow:

(a) Glass-formability variation to quench the phase-separated melts under a high temperature (Fraction follows the lever rule of phase equilibrium.)

(b) Possibility of obtaining novel glass ceramics with a high-temperature crystal phase.

Here, the frozen sorbet technique was applied to the SrO–Al_2O_3–B_2O_3 ternary system in order to prepare crystal–glass composites composed of $SrAl_2O_4$ crystals. **Figure 1**(a) shows a specific ternary diagram indicating the glass-forming region of the SrO–Al_2O_3–B_2O_3 system, which was taken from an international glass database (INTERGLAD Ver. 7, produced by New Glass Forum, Japan),[30] and an obtained sample picture is shown in Fig. 1(b). The composition of $54SrO–27Al_2O_3–19B_2O_3$ was optimized on the basis of results of our previous study.[23] Small amounts of Eu_2O_3 and Dy_2O_3 (1 mol % for the main composition) were added as activator ions. As shown in Fig. 1(a), the composition is located outside the glass-forming region in the ternary system, and a perfectly homogeneous melt was obtained only at temperatures above 1650°C. The part-separated melt at around 1500°C consists of liquid and crystalline phases, and this kind of liquid–solid mixture was quenched to room temperature, leading to the formation of a glass composite consisting of the target crystal. Actually, the crystal size, crystallinity, and crystal/glass-ratio, which is directly linked to the optical properties, can be controlled by melt conditions. In the case of the conventional heat-treatment technique for bulk glass, single precipitation of $SrAl_2O_4$ crystals could not be demonstrated because the precipitation of other crystal phases with a low-melting temperature such as SrB_2O_4 and $SrAl_2B_2O_7$[31] preferentially occurred, and their glass appearance became opaque due to phase separation in the glass matrix.

The frozen sorbet technique is similar to the flux technique for preparation of mono-crystals such as ruby (Cr^{3+}: Al_2O_3).[32] In the flux technique, well-controlled mono-crystals of millimeter-sized particles are formed from liquids of flux agents. In the case of liquid reaction, Ostwald ripening mainly controls the crystal size in the phase-separated melts. Consequently, the glass composite can be prepared by quenching of the phase-separated liquid. In a previous study, Ueda et al.[24] used a method similar to the frozen sorbet technique to fabricate an impressive glass composite with a mono-crystal phase of ruby rods (Cr^{3+}: α-Al_2O_3). It has been extremely difficult to precipitate single Al_2O_3 phase (e.g., corundum) in the glass matrix since Al-ions easily react with other components and form different compounds. In the case of the frozen sorbet technique, however, since crystal compounds except for Al_2O_3 (m.t. at 2050°C) were melted at 1550°C and the part-separated melts formed a glassy phase, the composite (glass + α-Al_2O_3) was obtained according to the lever rule of phase equilibrium. Material design of glass composites using the frozen sorbet technique shows might lead to new glass ceramics applications.

3. Structural features of Eu^{2+}: $SrAl_2O_4$-based glass composites

Crystal glass composites are light green in color and highly transparent [see Fig. 1(b)]. The diffuse transmittance of the glass composites is approximately about 75% at 510 nm and 50% at 400 nm.[23] The **Fig. 2** shows (a) an SEM image and (b) a polarization microscope image of $SrAl_2O_4$ glass composites. In the obtained glass composites, no large cracks were observed which could produce light scattering. Electron probe microanalysis (EPMA)-mapping images are also shown in Fig. 2(c). Polygonal $SrAl_2O_4$ microcrystals with diameters of ca. 30 µm can be seen. The polarized microscope image in Fig. 2(b) shows that each crystal has a mono-domain of the $SrAl_2O_4$ phase with various crystal planes. The glassy composite consisted of $SrAl_2O_4$ crystal phase (monoclinic, space group $P2_1$, ICDD 34-0379) and aluminoborate glass phase. The refraction index difference between crystal and glass phases was mainly observed depending on the concentration difference of the heaviest ions (e.g. Sr-ions) of the components. The negative index of the glass sample, which has similar Sr- amounts with $54SrO–27Al_2O_3–19B_2O_3$

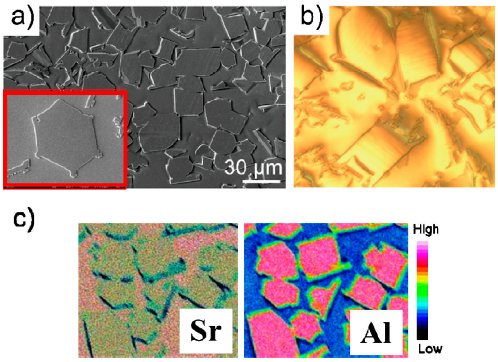


Fig. 2. (a) SEM image and (b) optical-polarized microscope image of the $SrAl_2O_4$ crystal–glass composite and (d) elemental distribution mapping for Sr and Al ions using EPMA.

system, was measured at around 1.73, and $SrAl_2O_4$ (single crystal) was 1.75 by the laser prism-coupling method. Thus, it can be thought that the obtained crystal glass composites could keep transparency in spite of the large crystal precipitations with several decade micro orders.[22] In the fabrication of composite materials consisting of a glassy phase and crystals obtained by using the frozen sorbet technique, the glass-forming region and the phase diagram for a given system are very important.[22] So far, there has been no report on the fabrication of glass ceramics containing only $SrAl_2O_4$ crystals using conventional heat-treatment processing in an electric furnace. The present study provided evidence that the frozen sorbet technique is a suitable technique for the preparation of $SrAl_2O_4$ glass composite in the $SrO–Al_2O_3–B_2O_3$ system. As supporting data, Fig. 2(c) shows compositional mapping images for the main component atoms: Sr and Al. The Sr ions showed a homogeneous distribution despite $SrAl_2O_4$ crystal precipitations. On the other hand, the Al ions were concentrated into the crystal sites. Generally, boron ions cannot be detected quantitatively by EPMA; however, we could predict concentrated boron in the glass phase on the basis of distributions of the other ions such as Al ions. It is obvious that the component of B_2O_3, which is classified as "glass network formers", enhances formation of the glassy phase. The present results indicate that $SrAl_2O_4$ crystals are frozen in the glassy phase during the quenching of melts. The author previously reported that a large amount of boron ions substituted into aluminum sites in the $SrAl_2O_4$ lattice leads to improvement of e light-storage ability.[22] The frozen sorbet technique can be used to prepare $SrAl_2O_4$ crystals with many impurity ions such as boron ions, which affect the light-storage properties[33),34)]

4. Photo-functional properties of Eu^{2+}: $SrAl_2O_4$-based glass ceramics

The author have reported that notable light-storage abilities strongly depend on the valence states of europium ions (Eu^{2+} or Eu^{3+}).[23] Long-persistent luminescence is well known as an efficient use for stored light energy. **Figures 3**(a) and 3(b) show a picture of Eu^{2+} luminescence under a mercury UV lamp ($\lambda =$ 365 nm) excitation and its long-persistent luminescence of the $SrAl_2O_4$ glass composite that was prepared under a weak reducing atmosphere ($P_{O2} = 10^{-8}$) using a high-temperature vacuum furnace. Green emission that peaked at 520 nm can be recognized a few hours later by the naked eye. A photoluminescence (PL) spectrum of the Eu^{2+}, Eu^{3+} and Dy^{3+}: $SrAl_2O_4$ glass composite under excitation at 393 nm (Eu^{2+} [$4f$ ($^8S_{7/2}$)–$4f5d$ (T_{2g})], Eu^{3+} [$4f$ ($^7F_0$)–$4f$ ($^5L_6$)], and Dy^{3+} [$4f$ ($^6H_{15/2}$)–$4f$ ($^4I_{13/2}$)] is shown in

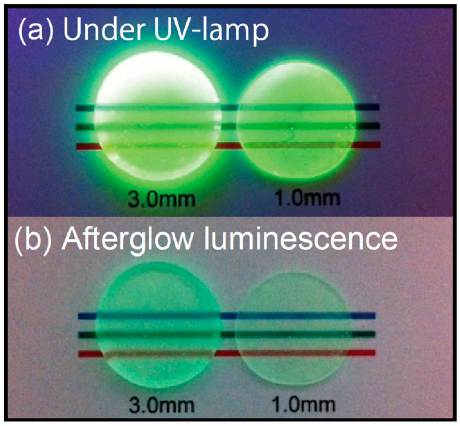


Fig. 3. Photo-image of (a) steady-state luminescence of Eu, Dy: $SrAl_2O_4$ crystal glass composite under mercury UV lamp excitation and (b) long-persistent (afterglow) luminescence after stopping excitation for 10 min.

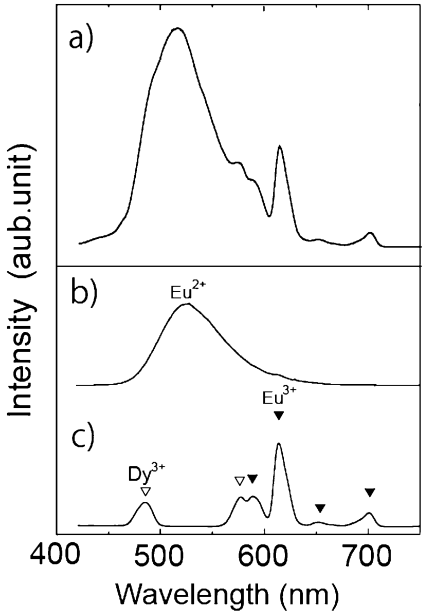


Fig. 4. Steady-state luminescence spectra for (a) Eu, Dy: $SrAl_2O_4$ crystal glass composite under excitation at 393 nm. Luminescent spectra of (b) Eu^{2+}:$SrAl_2O_4$ and (c) Eu^{3+}, Dy^{3+} in prepared pure borate glass (pure glassy) are shown in the same figure under excitation at 393 nm.

Fig. 4(a). As a base luminescence for comparison, the photoluminescence of (b) Eu^{2+}: $SrAl_2O_4$ and that of (c) Eu^{3+}, Dy^{3+}-codoped borate glass are shown in the same figure. The broadest emission band at around 520 nm can be assigned to the $4f$–$5d$ transition of Eu^{2+} ions in the $SrAl_2O_4$ crystalline phase for (a) and (b). The PL peaks of (a) at 590, 612, 650, and 700 nm are assigned to electronic transitions of Eu^{3+}: $^5D_0$–^7F_j (j = 1–4), while those at 485 and 575 nm are assigned to the transitions in Dy^{3+}: $^4F_{9/2}$–^6H_j (j = 15/2, 13/2). The $4f$–$4f$ transitions of Eu^{3+} and Dy^{3+} ions in a crystal matrix generally have narrow emission bands (FWHM < 5 nm); however, relatively broad $4f$–$4f$ emission bands are evident in Figs. 4(a) and 4(c) (FWHM > 10 nm), indicating that Eu^{3+} and Dy^{3+} ions are mainly present in the aluminoborate glass phase.[35),36)] **Figure 5** shows cathodeluminescence (CL)-mapping images at (a) 520 nm, (b) 612 nm and (c) image composition (a) and (c) for obtained samples. An SEM

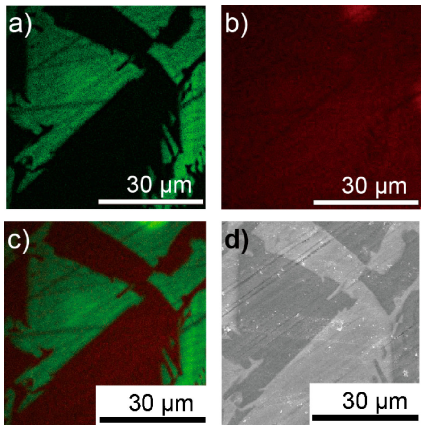


Fig. 5. Cathodeluminescence images at (a) 520 nm, (b) 612 nm and (c) image composition (a) and (c). SEM image at the same position is also shown in (d).

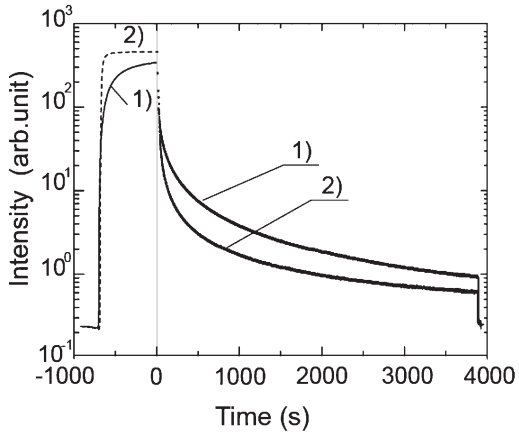


Fig. 6. Long-persistent luminescence curves of 1) Eu, Dy: $SrAl_2O_4$ crystal glass composite and 2) Eu, Dy: $SrAl_2O_4$. (Ex. = 390 nm, 30 min).

image at the same position is also shown in Fig. 5(d). The CL-mapping images suggest that Eu^{2+} ions are mainly located in the $SrAl_2O_4$ crystals, while Eu^{3+} ions are dispersed in both phases homogeneously. The Eu^{2+} ions are generally stabilized at Sr^{2+}-sites of $SrAl_2O_4$ crystals compared to that of glass phase due to charge compensation. From these results, it was concluded that Eu^{2+}, Dy^{3+}: $SrAl_2O_4$ microcrystals in aluminoborate glass with Eu(III) ions were successfully prepared using the frozen sorbet technique under P_{O2} control.[23)]

In order to compare the long-persistent luminescence properties, afterglow decay curves for the $SrAl_2O_4$ glass composite and a commercialized long-persisting phosphor (LumiNova/G300M, Nemoto & Co., Ltd.) are shown in **Fig. 6**. In this experiment, the intensity of PL at 520 nm after light irradiation (excitation at 390 nm for 30 min) was monitored as a function of time. It was seen that the decay time in $SrAl_2O_4$ glass ceramics is similar to that of the commercial product. Thermoluminescence (TL) measurements of the $SrAl_2O_4$ glass composite and Eu^{2+}, Dy^{3+}: $SrAl_2O_4$ ceramic plate were conducted to clarify the electron trap and de-trap mechanism linked to the light storage properties. The TL spectra are shown in **Fig. 7**. The TL spectra of the glass composite and Eu^{2+}, Dy^{3+}: $SrAl_2O_4$ were decomposed by curve fitting with a Gaussian function. Three characteristic bands were observed in the TL spectrum of the glass composite, whereas only one broad band was evident in the spectrum of the poly-

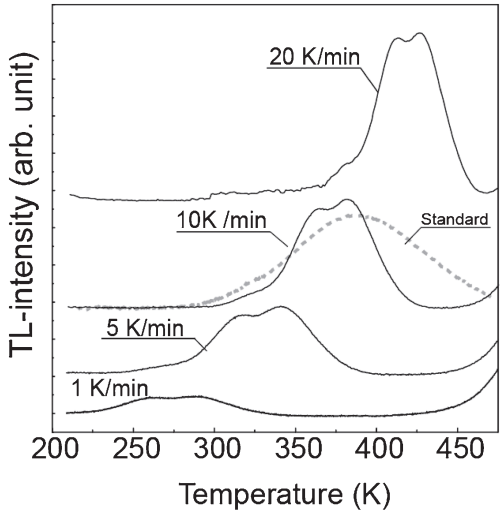


Fig. 7. TL spectrum monitored at 520 nm over the temperature range of 100–500 K for Eu, Dy: $SrAl_2O_4$ crystal glass composite. Temperature scan rates were 1, 5, 10, and 20 K/min. A TL curve of polycrystalline Eu, Dy: $SrAl_2O_4$ is also shown in the same figure as a standard for comparison (10 L/min).

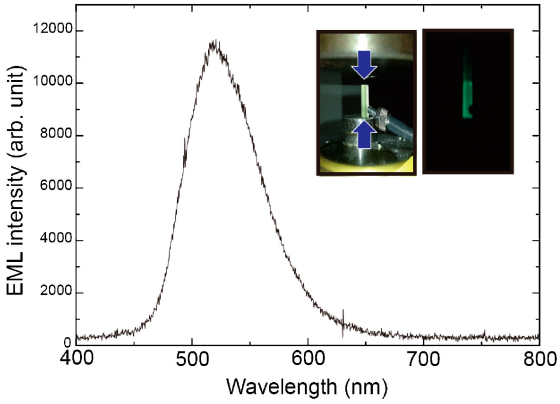


Fig. 8. Elastico-mechanoluminescence (EML) spectrum of Eu, Dy: $SrAl_2O_4$ crystal glass composite.

crystalline Eu^{2+}, Dy^{3+}: $SrAl_2O_4$ ceramic plate. We can estimate three exact trap sites in the Eu^{2+}, Dy^{3+}: $SrAl_2O_4$ glass composite, although the one broad band TL peak for the ceramic plate does not provide information regarding the energy levels of trap sites. Here, the trap-energy levels can be estimated in a simple way.[37),38)] The activation energies (660, 700, and 760 meV) for the glass composite were estimated from three peaks with narrow full-width at half maxim (FWHM). The activation energy (740 meV) for polycrystalline Eu^{2+}, Dy^{3+}: $SrAl_2O_4$ was obtained from the one broad peak in the spectrum.[39)] In polycrystalline Eu^{2+}, Dy^{3+}: $SrAl_2O_4$, the trap levels are continuously distributed over a wide range of energies (as evidenced by the extremely broad TL band). In contrast, the glass composite exhibits three distinct trap levels linked to the long-persisting luminescence properties. The narrow dispersion of trap levels can be controlled by the type of doping elements.[33)]

Unique elastico-mechanoluminescence (EML) in light-storage materials is also known as one of the ways for efficient use used of stored light-energy.[40),41)] **Figure 8** shows an EML spectrum of Eu^{2+}, Dy^{3+}: $SrAl_2O_4$ glass composites subjected to a compressive load (5 mm/min, 5000 N for 15 mm^2). The inset pictures are

EML photo-images before and after the compressive load. Green emission that peaked at 520 nm, which is the same as PL of Eu^{2+}: $SrAl_2O_4$, was observed from the glass-ceramics rod (5 × 3 × 30 mm) homogenously, and the emission intensity of EML increased monotonically depending on the force of the compressive load. One of the notable aspects is that applied force can be loaded into the crystals without loss due to their hardness based on glass ceramic properties, and the transparency like a mono-crystal leads to effective light extraction. Currently, many research groups[40)–42)] assume that the EML phenomenon can be explained by the de-trapping model of storage charge carriers (electrons or holes) using a mechanical stimulus. Thus, the trap levels play an important role in the EML process, which is similar to the design of long-persistent luminescence materials.

These remarkable results suggest that from the viewpoint of notable light-storage ability, the $SrAl_2O_4$ glass composite prepared using the frozen sorbet technique has some advantages, such as transparency, chemical durability and formability, based on glass ceramic properties compared with polycrystalline: Eu^{2+}, Dy^{3+} $SrAl_2O_4$, which is already in use. Green emission that peaked at 520 nm can be recognized after a few hours by the naked eye and, more importantly, the hardness and transparency as a glass composite is attractive for many applications. In view of the material chemistry, results of further studies on the Eu^{2+}, Dy^{3+}: $SrAl_2O_4$ glass composite should contribute to the development of future light-storage materials as advanced materials.

5. Conclusion

The preparation of lanthanide-activated crystal glass composites with photo-functionalities is briefly reviewed. A transparent $SrAl_2O_4$ glass composite with light-storage ability was successfully prepared from an SrO–Al_2O_3–B_2O_3 glass system by using the frozen sorbet technique. It was found that $SrAl_2O_4$ crystals in the glass composite show excellent persistent luminescence and elastico-mechanoluminescence based on their light-storage ability of Eu^{2+}-activated $SrAl_2O_4$. It is expected that the notable glass ceramics with light-storage ability will lead to the new glass ceramic applications.

Acknowledgement The author wishes to thank all of the coworkers who supported him. Most of the coworkers are listed as coauthors in the references. In particular, the author wishes to thank his supervisors, Prof. Setsuhisa Tanabe (Kyoto University), Prof. Takayuki Komatsu (Nagaoka University), and Prof. Yasuchika Hasegawa (Hokkaido University), for their critical ideas and great support. The author also thanks T. Murakami (Shimadzu Co.) for his technical assistance in EML measurements. This work was partly supported by the Nippon Sheet Glass Foundation for Materials Science and Murata Science Foundation.

References

1) S. Tanabe, S. Fujita, A. Sakamoto and S. Yamamoto, *Ceram.Trans*, 173, 19–23 (2006).
2) B. M. Ende, L. Aarts and A. Meijerink, *Phys. Chem. Chem. Phys.*, 11, 11081–11095 (2009).
3) S. Okamoto and E. Nakazawa, *Jpn. J. Appl. Phys.*, 34, 521–526 (2005).
4) G. Blasse, *Chem. Mater.*, 6, 1465–1475 (1994).
5) A. Bessière, S. K. Sharma, N. Basavaraju, K. R. Priolkar, L. Binet, B. Viana, A. J. J. Bos, T. Maldiney, C. Richard, D. Scherman and D. Gourier, *Chem. Mater.*, 26, 1365–1373 (2014).
6) Z. Pan, Y-Y. Lu and F. Liu, *Nat. Mater.*, 11, 58–63 (2012).
7) H. Hölsä, *Electrochem. Soc. Interf.*, 18, 42–45 (2009).
8) A. Stevenson, A. Jobes and S. Raghavan, *Nano Lett.*, 11, 3274–3278 (2011).
9) N.-C. Xu, T. Watanabe, M. Akiyama and X. G. Zheng, *Appl. Phys. Lett.*, 74, 2414–2416 (2009).
10) F. Clabau, X. Rocquefelte, S. Jobic, P. Deniard, M.-H. Whangbo, A. Garcia and T. L. Mercier, *Chem. Mater.*, 17, 3904–3912 (2005).
11) F. Clabau, X. Rocquefelte, T. L. Mercier, P. Deniard, S. Jobic and M.-H. Whangbo, *Chem. Mater.*, 18, 3212–3220 (2006).
12) J. Xu, J. Ueda and S. Tanabe, *Opt. Mater. Exp.*, 5-5, 963–968 (2015).
13) K. V. Eeckhout, P. F. Smet and D. Poelman, *Materials (Basel)*, 3, 2536–2566 (2010).
14) J. Xu, J. Ueda, K. Kuroishi and S. Tanabe, *Scr. Mater.*, 102, 47–50 (2015).
15) T. Matsuzawa, Y. Aoki, N. Takeuchi and Y. Murayama, *J. Electrochem. Soc.*, 143, 2670–2673 (1996).
16) P. Dorenbos, *J. Electrochem. Soc.*, 152, 107–110 (2005).
17) J. Chen, F. Cu and C. Li, *Cryst. Growth Des.*, 8, 3175–3179 (2008).
18) K. Y. Jung, H. W. Lee and H.-K. Jung, *Chem. Mater.*, 18, 2249–2255 (2006).
19) A. Nag and T. N. R. Kutty, *J. Alloys Compd.*, 354, 221–231 (2003).
20) T. Nakanishi and S. Tanabe, *IEEE J. Sel. Top. Quantum Electron.*, 15, 1171–1176 (2009).
21) T. Nakanishi and S. Tanabe, *Phys. Status Solidi A*, 206, 919–922 (2009).
22) T. Nakanishi, Y. Katayama, J. Ueda, S. Tanabe, T. Honma and T. Komatsu, *J. Ceram. Soc. Japan*, 119, 609–615 (2011).
23) T. Nakanishi, K. Watanabe, J. Ueda, K. Fushimi, S. Tanabe and Y. Hasegawa, *J. Am. Ceram. Soc.*, 98, 423–429 (2015).
24) J. Ueda and S. Tanabe, *J. Am. Ceram. Soc.*, 93, 3084–3087 (2010).
25) S. Fujita and S. Tanabe, *Opt. Mater.*, 32, 886–890 (2010).
26) P. Dorenbos, *J. Lumin.*, 104, 239–260 (2003).
27) Inorganic phosphors, Ed. by W. M. Yen, and M. J. Weber, CRC Press (2004).
28) J. K. Park, M. A. Lim, C. H. Kim and H. D. Park, *Appl. Phys. Lett.*, 82, 683–685 (2003).
29) T. L. Barry, *J. Electrochem. Soc.*, 115, 1181–1184 (1968).
30) Glass Data-Base InterGlad, http://www.newglass.jp/c2j.shtml, produced by New Glass Form, Japan.
31) Y. Yu and B. Kim, *Korean J. Chem. Eng.*, 20, 973 (2003).
32) S. Oishi, K. Teshima and H. Kondo, *J. Am. Chem. Soc.*, 126, 4768–4769 (2004).
33) T. Katsumata, S. Toyomane, R. Sakai, S. Komuro and T. Morikawa, *J. Am. Ceram. Soc.*, 89, 932–936 (2006).
34) K. Y. Jung, H. W. Lee and H.-K. Jung, *Chem. Mater.*, 18, 2249–2255 (2006).
35) S. Tanabe, H. Hayashi, T. Hanada and N. Onodera, *Opt. Mater.*, 19, 343–349 (2002).
36) S. Tanabe, J. Kang, T. Hanada and N. Soga, *J. Non-Cryst. Solids*, 239, 170–175 (1998).
37) J. T. Randall and M. H. F. Wilkins, *Proc. R. Soc.*, A184, 366–389 (1945).
38) V. Viana, T. Maldiney, S. Blahuta, A. Béssière, D. Gourier, C. Richard, D. Scherman and V. Ouspenski, *Proc. SPIE*, 8626, 86260R (2013).
39) H. Takasaki, S. Tanabe and T. Hanada, *J. Ceram. Soc. Japan*, 104, 322–327 (1995) [in japanese].
40) J.-C. Zhang, C.-N. Xu and Y.-Z. Long, *Opto. Exp.*, 21, 13699–13709 (2013).
41) V. K. Chandra and B. P. Chandra, *J. Lumin.*, 132, 858–869 (2012).
42) J. Botterman, K. V. Eeckhout, I. D. Baere, D. Poelman and P. F. Smet, *Acta Mater.*, 60, 5494–5500 (2012).



Takayuki Nakanishi received a Ph.D. from the Kyoto University, Kyoto, Japan, in 2010. He was as a Research Fellowship for Young Scientists of JSPS at the Graduate School of Human and Environmental Studies, Kyoto University in 2009, and Materials Science and Technology, Nagaoka University of Technology in 2010. Since 2011, he has been performing research as an Assistant Professor at the Faculty of Engineering, Hokkaido University.